Morphological Control of Rod- and Fiberlike SBA-15 Type Mesoporous Silica Using Water-Soluble Sodium Silicate

Katsunori Kosuge,* Tetsu Sato, Nobuyuki Kikukawa, and Makoto Takemori

Catalyst Development Group, Research Institute for Green Technology, National Institute of Advanced Industrial Science and Technology, 16-1 Onogawa, Tsukuba-shi, Ibaraki, 305-8569 Japan

Received September 29, 2003. Revised Manuscript Received December 31, 2003

Well-defined rodlike and fiberlike SBA-15 mesoporous silicas have been selectively synthesized from an aqueous reaction mixture consisting of a commercial sodium silicate solution, P123 triblock copolymer and HCl. The morphologies and physicochemical properties of the products were found to be greatly affected by the shearing stress exerted by cylindrical silicated-surfactant micelles in a flowing solution, referred to hereafter as "shearing flow". Monodispersed rodlike particles ca. 0.5-μm wide and ca. 1−2-μm long were formed under static reaction conditions, whereas continuous stirring of the reaction mixture led to the formation of fiberlike silicas with lengths of several hundred micrometers and a relatively uniform width of ca. 10 μm. The effects of the synthesis conditions, such as the initial ratio of the reactants, time, temperature, and the acid source, in addition to shearing flow, on particle morphologies were investigated. Fiberlike silicas of various lengths were obtained from a relatively wide range of synthesis conditions, while monodispersed rodlike silicas were prepared under very specific conditions. Each fiberlike product was found to be comprised of a bundle of fibers, with each fiber formed by the coupling of rodlike particles of almost identical size, irrespective of different synthesis conditions.

Introduction

One of the main areas of interest in materials chemistry is the synthesis of mesoporous molecular sieves with highly controllable morphologies for the purpose of providing catalytic, separation, and adsorption applications to industry. Nonionic templates such as poly(ethylene oxide) (PEO) and block copolymers have received a great deal of attention in the synthesis of mesoporous materials[1,2] because of their ability to self-assemble into well-defined mesophases with crystalline-like long-range orders.[3−5] Furthermore, such nonionic surfactants are easily separated, nontoxic, biodegradable, and relatively inexpensive. The $[S^0H^+][X^-I^+]$ assembly pathway using block copolymer templating has resulted in various morphological mesoporous silicas[6−13] arising from weak interface interactions mediated by the X^- anions under acidic conditions, like in the $S^+X^-I^+$ assembly pathway using a cationic surfactant.[14] Recent studies have reported well-defined morphological mesoporous silicas such as films,[6] monoliths,[7] spheres,[8,9] fibers,[6,10] and rodlike powders.[9,11,12] However, the synthesis procedures for preparing these products require relatively expensive inorganic precursors, such as tetraethoxysilane (TEOS).

Sierra and Guth first reported a synthesis method using low-cost sodium silicate in place of costly silicon alkoxides as a silica source with a nonionic poly(ethylene oxide) surfactant. The products of this method exhibited low thermal stability.[15] Some research groups have prepared thermally stable mesoporous silica products using sodium silicate solutions by block copolymer templating. Examples include MSU-X with wormlike porous structures,[16] various SBA-type mesoporous silicas with highly ordered mesophases,[17] and large meso-

* To whom correspondence should be addressed. Telephone: +81-29-861-8492. Fax: +81-29-861-8459. E-mail: k.kosuge@aist.go.jp.

(1) Bagshaw, S. A.; Prouzet, E.; Pinnavaia, T. J. *Science* **1995**, *269*, 1242.
(2) (a) Zhao, D.; Feng, J.; Huo, Q.; Melosh, N.; Fredrickson, G. H.; Chmelka, B. F.; Stucky, G. D. *Science* **1998**, *279*, 548. (b) Zhao, D.; Huo, Q.; Feng, J.; Chmelka, B. F.; Stucky, G. D. *J. Am. Chem. Soc.* **1998**, *120*, 6024.
(3) Wanka, G.; Hoffmann, H.; Ulbricht, W. *Macromolecules* **1994**, *27*, 4145.
(4) Alexandridis, P.; Hatton, T. A. *Colloids Surf., A* **1995**, *96*, 1.
(5) Mortensen, K. *Polym. Adv. Technol.* **2001**, *12*, 2.
(6) (a) Zhao, D.; Yang, P.; Meiso, N.; Feng, J.; Chmelka, B. F.; Stucky, G. D. *Adv. Mater.* **1998**, *10*, 1380. (b) Miyata, H.; Noma, T.; Watanabe, M.; Kuroda, K. *Chem. Mater.* **2002**, *14*, 766.
(7) Feng, J.; Bu, X.; Stucky, G. D.; Pine, D. J. *J. Am. Chem. Soc.* **2000**, *122*, 994.
(8) Zhao, D.; Sun, J.; Li, Q.; Stucky, G. D. *Chem. Mater.* **2000**, *12*, 275.
(9) Boissière, C.; Larbot, A.; van der Lee, A.; Kooyman, P. J.; Prouzet, E. *Chem. Mater.* **2000**, *12*, 2902.
(10) Yang, P.; Zhao, D.; Chmelka, B. F.; Stucky, G. D. *Chem. Mater.* **1998**, *10*, 2033.
(11) Schmidt-Winkel, P.; Yang, P.; Margolese, D. I.; Chmelka, B. F.; Stucky, G. D. *Adv. Mater.* **1999**, *11*, 303.
(12) Yu, C.; Fan, J.; Tian, B.; Zhao, D.; Stucky, G. D. *Adv. Mater.* **2002**, *14*, 1742.
(13) (a) Ciesla, U.; Schüth, F. *Microporous Mesoporous Mater.* **1999**, *27*, 131. (b) Leontidis, E. *Curr. Opin. Colloid Interface Sci.* **2002**, *7*, 81.
(14) (a) Lin, H. P.; Liu, S. B. Mou, C. Y.; Tang, C. Y. *Chem. Commun.* **1999**, 583. (b) Lin, H. P.; Kao, C. P.; Mou, C. Y.; Liu, S. B. *J. Phys. Chem. B* **2000**, *104*, 7885.
(15) Sierra, L.; Guth, J.-L. *Microporous Mesoporous Mater.* **1999**, 28, 243.

10.1021/cm030622u CCC: $27.50
Published on Web 02/06/2004

Table 1. Reaction Conditions and Physicochemical Properties of Representative SBA-15 Type Mesoporous Silicas

sample name[a]	temp. °C	molar ratio[b] HCl	P123	H_2O	induction time[c] (min)	S_{BET}[d] (m^2/g)	V_{meso}[e] (mL/g)	V_{micro}[f] (mL/g)	D_{meso}[g] (nm)	d_{001}[h] (nm)	particle morphologies
RA	30	5.90	0.017	203	9.5	430	0.46	0.02	5.46	7.89	monodispersed rod
FA	30	5.90	0.017	203		730	0.63	0.12	5.62	8.27	fiber
RB	30	4.41	0.017	204	16.5	586	0.58	0.06	5.96	8.19	solid [i]
FB	30	4.41	0.017	204		851	0.72	0.15	5.96	7.74	short fiber
RC	30	7.32	0.017	202	6.7	757	0.65	0.11	5.84	8.10	monodispersed rod
FC	30	7.32	0.017	202		689	0.58	0.11	5.64	7.97	short fiber
RD	30	5.90	0.013	202	5	563	0.47	0.08	5.30	8.16	agglomerated particles[j]
FD	30	5.90	0.013	202		766	0.57	0.14	5.14	8.10	short fiber
RE	30	5.90	0.021	202	18	543	0.58	0.02	5.96	7.77	solid[i]
FE	30	5.90	0.021	202		911	0.78	0.17	6.20	7.85	short fiber
RF	30	3.92	0.017	152	8.5	651	0.59	0.08	5.87	8.26	agglomerated particles[j]
FF	30	3.92	0.017	152		818	0.69	0.15	5.90	8.26	fiber[k]
RG	30	7.84	0.017	252	13	747	0.56	0.12	5.97	7.96	monodispersed rod
FG	30	7.84	0.017	252		897	0.76	0.16	6.08	7.85	fiber
RH	25	5.90	0.017	201	13.5	697	0.61	0.08	5.44	7.89	agglomerated particles [j]
FH	25	5.90	0.017	201		803	0.64	0.13	5.40	8.10	agglomerated particles[l]
RI	40	5.90	0.017	202	5	578	0.57	0.08	6.34	8.56	agglomerated particles[j]
FI	40	5.90	0.017	202		835	0.72	0.14	6.78	8.58	fiber

[a] Sample names are denoted by combinations of two letters. An identical combination indicates that the products were obtained using the same reactant mixture; R and F differentiate the stirring state, without stirring and with stirring, respectively. [b] The molar ratio of reactants with respect to SiO_2. [c] Induction time was almost identical with or without stirring when synthesized under the same reaction-mixing ratio at a defined reaction temperature. [d] S_{BET}, BET surface area. [e] V_{meso}. [f] V_{micro} are primary mesoporous and microporous volumes evaluated by the t-plot method, respectively. [g] $D_{meso}$is the BJH mesopore diameter calculated from the adsorption branch. [h] $d_{001}$is the XRD *d* spacing. [i] Densely packed solids composed of rodlike particles (see Figure 3c,d). [j] Loosely packed particles composed of short rodlike ones (see Figure 3e). [k] Well-defined fibrous silica coexisting with entangled and agglomerated particles composed of rodlike ones (see Figure 3f). [l] Agglomerated particles comprising rodlike ones (see Figure 3f).

porous MSU-H products with two-dimensional (2D) hexagonal structures.[18]

However, only a few studies have addressed the synthesis of well-defined, morphologically controlled products that exist as monodispersed particles using a low-cost silica source by block copolymer templating.[19,20] Spheroidal and short rodlike particles were synthesized by adjusting the polycondensation rate of silicic acids by changing the pH and reaction temperature, but the resultant products had a lower order of monodispersity and low thermal stability.[19] MSU-X type mesoporous spherical particles with a highly specific surface area were prepared using a two-step synthesis pathway by separating the assembly step from the condensation step in slightly acidic conditions.[20]

The morphology of particles and mesostructures generated by the $[S^0H^+][X^-I^+]$ pathway can be greatly affected by inorganic salts.[8,9,11,12,21] Mesoporous rodlike particles were first synthesized using sodium metasilicate as a silica source with a cationic surfactant. This reaction produced agglomerated solids of rodlike particles.[22] Such rodlike particles have been obtained using TEOS and a nonionic triblock copolymer of Pluronic P123 through the addition of inorganic fluoride salts[9,11] and KCl followed by post-hydrothermal treatment.[12] Sodium silicate is believed to act as both a silica source and inorganic salt in the formation of rodlike mesoporous silicas. The present work describes the selective formation of SBA-15 mesoporous silicas with well-defined macroscopic morphologies of rods and fibers using sodium silicate and P123 as the starting materials. Our rodlike products were obtained with higher uniformity and monodispersity under quiescent conditions than those of conventional synthesis methods. We found that fiberlike silicas are formed by the coupling of uniformly sized rodlike particles irrespective of different synthesis conditions. Additional information on the formation processes of rodlike and fiberlike silicas is discussed briefly on the basis of SEM and TEM observations.

Experimental Section

Materials Synthesis. Mesoporous SBA-15 silicas were synthesized by using triblock copolymer, Pluronic P123 (EO_{20}-$PO_{70}EO_{20}$) (hereafter, P123), as a template and a sodium silicate solution (SiO_2 23.6%, Na_2O 7.59%) as a silicate source under acidic conditions. All commercial chemicals were used without purification. A sodium silicate solution, more dilute than that outlined above, and P123 dissolved in an aqueous solution of HCl, HNO_3, HBr, or H_2SO_4 were kept separately at the desired temperature. The reaction stoichiometry used here was 1.0:0.013−0.022:2.45−7.85:110−250 SiO_2:P123:acid:H_2O. Amounts of the inorganic salts were identical: $Na_2O/SiO_2 = 0.312$. There were no precipitates in any of the reaction mixtures without the addition of P123 under the present conditions. In a typical synthesis (RA and FA in Table 1), 2 g of P123 was dissolved in 60 g of 2 mol/L HCl. Then, this mixture was added quickly to a mixture of 5.2 g of the sodium silicate solution and 15 g of deionized water at 30 °C with a magnetic stirrer at 600 rpm. For rodlike silica, stirring was stopped after 30 s and the reaction solution was subsequently kept under static conditions for a specified time. In contrast, for the fiberlike silica, the reaction solution was continuously stirred to completion. Immediately after rapid mixing of both solutions with stirring, the interaction between the silica

(16) Kim, S. S.; Pauly, T. R.; Pinnavaia, T. J. *Chem. Commun.* **2000**, 835.
(17) Kim, J. M.; Stucky, G. D. *Chem. Commun.* **2000**, 1159.
(18) (a) Kim, S. S.; Pauly, T. R.; Pinnavaia, T. J. *Chem. Commun.* **2000**, 1661. (b) Kim, S. S.; Karkamkar, A.; Pinnavaia, T. J.; Kruk, M.; Jaroniec, M. *J. Phys. Chem. B* **2001**, *105*, 7663. (c) Joo, S. H.; Ryoo, R.; Kruk, M.; Jaroniec, M. *J. Phys. Chem. B* **2002**, *106*, 4640.
(19) Sierra, L.; Lopes, B.; Guth, J.-L. *Microporous Mesoporous Mater.* **2000**, *39*, 519.
(20) Boissière, C.; Larbot, A.; Prouzet, E. *Chem. Mater.* **2000**, *12*, 1937.
(21) (a) Yu, C.; Tian, B.; Fan, J.; Stucky, G. D.; Zhao, D. *Chem. Commun.* **2001**, 2726. (b) Newalkar, B. L.; Komarneni, S. *Chem. Mater.* **2001**, *13*, 4573. (c) Yu, C.; Tian, B.; Fan, J.; Stucky, G. D.; Zhao, D. *J. Am. Chem. Soc.* **2002**, *124*, 4556.
(22) Shio, S.; Kimura, A.; Yamaguchi, M.; Yoshida, K.; Kuroda, K. *Chem. Commun.* **1998**, 2461.

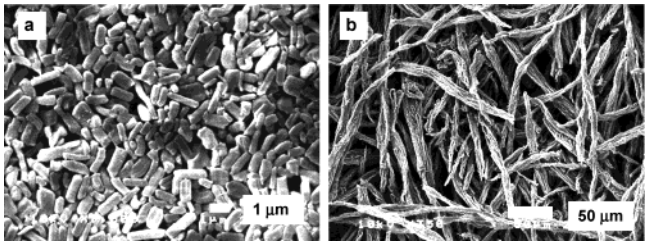

Figure 1. SEM micrographs of (a) rodlike silica of sample RA and (b) fiberlike silica of sample FA obtained at the basic reaction conditions without stirring and with stirring, respectively.

oligomers and the P123 micelles resulted in an emulsion.[23] A well-defined induction time before precipitation, during which the suspension was translucent, was observed under all reaction conditions. For rodlike silica, stirring was stopped after 30 s. The reaction mixture was subsequently kept under static conditions for a specified time. In contrast, for the fiberlike silica the reaction solution was continuously stirred. Both product yields were perfect on the basis of silica recovery for reaction times over 6 h. Reactions were run at 25, 30, 40, and 50 °C. Solid products were filtrated and washed repeatedly with warm deionized water. After drying at room temperature for 2 days and then at 50 °C for another 2 days, the products were calcined at 600 °C for 1 h in air.

Characterization. Powder X-ray diffraction (XRD) patterns were obtained with a Rigaku Rotaflex diffractometer equipped with a rotating anode using Cu Kα radiation. Scanning electron microscopy (SEM) images were obtained with JEOL5300 and Hitachi FE-SEM S-4700 microscopes. Transmission electron microscopy (TEM) images were obtained with a JEOL 2000FX microscope. N_2 sorption isotherms were obtained at −196 °C on a BELSORP 28 apparatus under continuous adsorption conditions. Samples were heated at 200 °C for 2 h and then outgassed to 10^{-3} Torr at room temperature prior to the N_2 sorption measurements. BET analysis was used to determine the total specific surface area (S_{BET}). The total pore volume (V_{total}) and micropore volume (V_{micro}) of products were calculated using a t-plot analysis.[24] The BJH method was used to calculate mesopore size distributions.

Results and Discussion

Stirring Effect. Among our various synthesis conditions, the mole composition of 1:0.017:5.90:203 SiO_2:P123:HCl:H_2O was found to be the optimum mixing ratio for the preparation of both rodlike and fiberlike silicas. The reactions were typically run at 30 °C for 6 h. We denote these synthesis conditions as the "basic synthesis conditions" or "basic reaction mixture", excluding the reaction temperature and time.

Figure 1 shows SEM images of samples RA and FA (sample names listed in Table 1 will be used hereafter in the text and figures) synthesized using the basic synthesis conditions. The two samples clearly exhibit completely different macroscopic morphologies depending on the use of continuous stirring during the reaction. Static conditions resulted in the formation of the monodispersed rodlike particles of sample RA with a relatively uniform size of ca. 0.5 μm in width and 1−2 μm in length (Figure 1a). On the other hand, the silica products obtained under continuous stirring were comprised of fiberlike silicas with lengths of several hundred micrometers and a relatively uniform width of ca. 10 μm (Figure 1b).

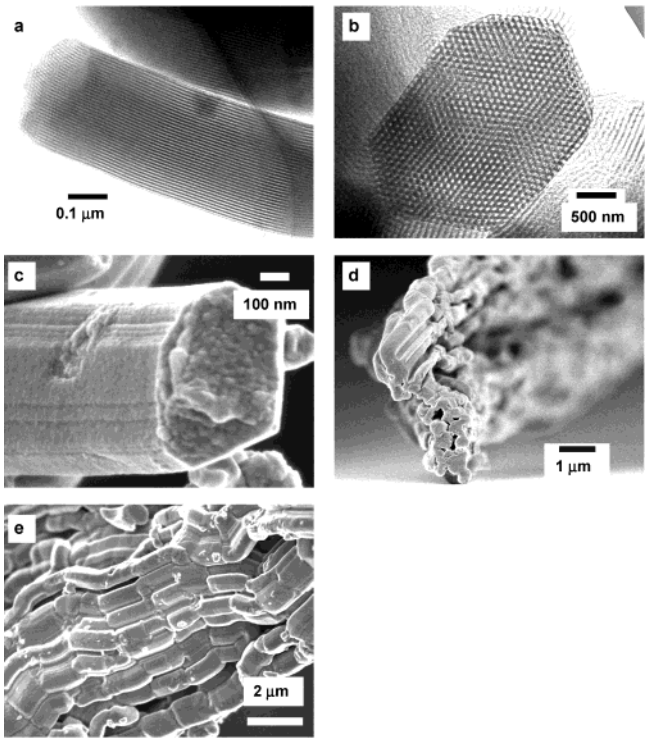

Figure 2. TEM micrographs of (a) rodlike sample RA and (b) that cross-sectional magnified image. (c) FE-SEM image of sample RA. FE-SEM micrographs of (d) a cross-sectional fiberlike sample FA and (e) its magnified image along the long axis.

Parts (a) and (b) of Figure 2 show the transmission electron microscopy (TEM) images of the rodlike particles of sample RA shown in Figure 1a. The image in Figure 2a shows that the rodlike particles form 1D mesoporous channels that are ca. 5 nm in diameter and run parallel to the long axis from one end to the other. The observed section shows that they are perfectly stacked to form a hexagon (Figure 2b). Figure 2c is an FE-SEM image of the rodlike particles along the long axis. We can observe many parallel stripes on the surface of the rodlike silicas, as with the SEM image. The parallel stripes in these images demonstrate regular stacking of elongated cylindrical $[S^0H^+][X^-I^+]$ assemblies of the synthesized rodlike particles. Pluronic P123 with longer PPO blocks, corresponding to a more hydrophobic molecule, has a stronger tendency to form elongated micelles.[3−5] Along with these intrinsic features of P123, coexisting inorganic sodium silicates consistently accelerate the formation of elongated cylindrical silicated-surfactant micelles.[21]

Figure 2d shows the cross section image of the fiberlike silicas of sample FB. The fiberlike products are clearly comprised of bundles of fibers, the cross sections of which are often hexagonal. The FE-SEM micrographs in Figure 2e show that each fiber is formed by coupling of the rodlike particles shown in Figure 1a.

It is clear from the results above that the macroscopic morphologies of the rodlike and fiberlike products are governed by the effects of stirring during their synthesis in acidic solutions of P123 triblock copolymer micelles. Stirring is the indispensable factor for fiberlike silica

(23) Boissière, C.; Larbot, A.; Bourgaux, C.; Prouzet, E.; Bunton, C. A. *Chem. Mater.* **2001**, *13*, 3580.

(24) (a) Gregg, S. G.; Sing, K. S. W. *Adsorption Surface Area and Porosity*, 2nd ed.; Academic Press: New York, 1982. (b) Sing, K. S. W.; Everett, D. H.; Haul, R. A. W.; Moscou, L.; Pierotti, R. A.; Rouquerol, J.; Siemienewska, T. *Pure Appl. Chem.* **1985**, *57*, 603.

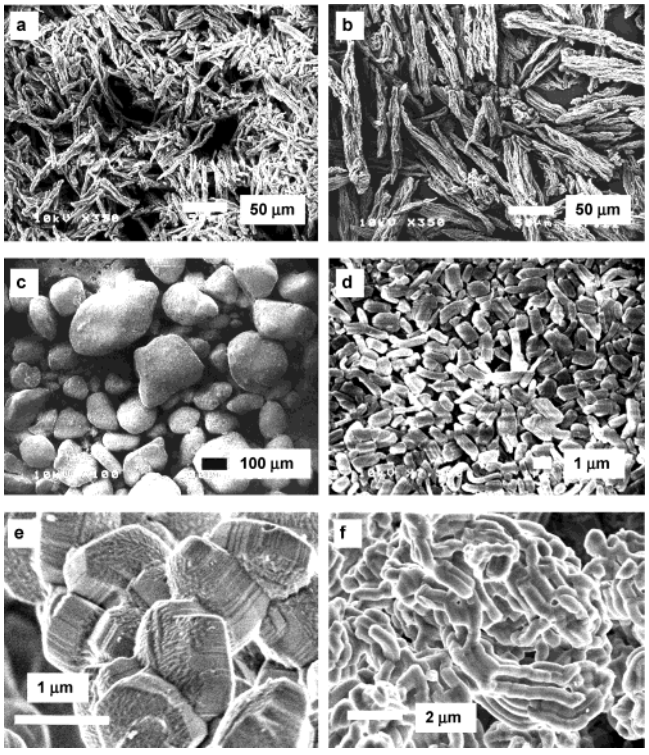

Figure 3. SEM micrographs of representative samples obtained at various reaction conditions: (a) short fiberlike silica of sample FC at high HCl concentration; (b) short and thick fibrous silica of samples FD with a small amount of P123; (c) densely aggregated solid of sample RB at low HCl concentration; and (d) solid surface of (c) composed of rodlike particles. FE-SEM micrographs of the sample prepared at 25 °C: (e) without stirring and (f) with stirring. The panel (e) shows a short rodlike silica of sample RH while not monodispersed and (f) entangled and densely packed particles composed of rodlike particles of sample FH.

formation in aqueous reaction systems, for example, fibrous SBA-15[8,11] and MCM-41.[14,25] On the other hand, various macroscopic morphologies such as spheres,[25] gyroidal spheres,[14,25] and rodlike particles[12,22] were formed under static conditions. In particular, our reaction method resulted in the first preparation of monodispersed rodlike particles, while every comparable system to date has resulted in an aggregated solid composed of many rodlike particles with 3D-network structures.[9,12,22] Our method uniquely allows for a simple selective synthesis of different macroscopic silicas from the same reaction mixture.

Effects of the Reaction Mixture Composition and Reaction Temperature. The effects of the synthesis reaction stoichiometry and reaction temperature on particle morphology were investigated by changing the basic synthesis conditions outlined earlier. Table 1 shows the representative reaction conditions and molar ratios of reactants with respect to SiO_2. The induction time is almost the same with or without stirring when the synthesis is performed using the same molar ratio at a defined reaction temperature. Figure 3 shows representative SEM images of the products. The SEM observations and the results in Table 1 revealed that small changes in the molar ratios created visible macroscopic morphological differences.

Table 1 shows that fiberlike silicas were obtained under a relatively wide variety of synthesis conditions (samples FB, FC, FD, FE, FF, FG, and FI), even in the cases in which agglomerated particles were formed under the corresponding static conditions. Hence, we were able to synthesize fiberlike silicas with different lengths and widths through careful control of the synthetic molar ratios, as shown in Figures 1b, 3a, and 3b. On the other hand, well-defined monodispersed rodlike silicas such as those shown in Figure 1a were prepared under a very narrow range of synthesis conditions without stirring (samples RC and RG). Some reactions under static conditions resulted in densely aggregated solids composed of rodlike particles (samples RB and RE), as shown in Figure 3c,d. Shorter cylindrical silicated-surfactant architectures generated under a wide range of reaction conditions resulted in the formation of short, aggregated rodlike particles (samples RD, RF, RH, and RI). Figure 3e shows these short rodlike particles with surfaces that display parallel stripes such as those depicted in Figure 2e.

Varying the temperature of our reaction system revealed that particle morphologies were highly sensitive to reaction temperature, even in a narrow region (25−50 °C). The fiberlike silica synthesized at 40 °C (sample FI) was the only comparable product in size and dispersity with the fiberlike product obtained under the basic synthesis conditions.

Observations by FE-SEM of the various fiberlike silicas synthesized in this study revealed that all of them are composed of connections between rodlike particles, as shown in Figure 2e (Supporting Information, Figure S-1). Structure units of primary rodlike particles can be seen even in the irregular solids obtained from some of the reactions with stirring, as shown in Figure 3f, which are aggregated into entangled and densely packed agglomerations. The original paper[2a] on SBA-15 reported nearly identical structural units of rodlike particles with a uniform size of ca. 1 μm that aggregated into wheatlike macroscopic particles, similar to the short fiberlike silicas in this work. Similar fiberlike structures were observed in other fiberlike SBA[8,11] and MSU[9] type materials and in fiberlike MCM-41. However, in this latter case, the primary rodlike particles seemed to have ill-defined morphologies rather than the uniform morphologies in other work.[14]

In contrast, every sample prepared in the broad reaction mixture range of 1.0:0.013−0.022:2.45−7.85:110−250 SiO_2:P123:HCl:H_2O had similar XRD patterns and sorption isotherms irrespective of different macroscopic morphologies (Supporting Information, Figures S-2 and S-3). Every silica had very intense (100) diffraction peaks and two or more well-resolved peaks (100, 110, 200), which are indexed as 2D hexagonal symmetry. Their sorption isotherms were of a IV type with an irreversible H1 hysteresis loop.[24] These XRD patterns and sorption isotherms were typical for SBA-15 that has an ordered array of cylindrical 1D channels,[2] indicating that products with primary rodlike particles as the structural unit have the same mesostructures.

Acid Source. In our synthesis, the use of the other acid sources (besides HCl) in the Experimental Section

(25) (a) Schacht, S.; Huo, Q.; Voigt-Martin, I. G.; Stucky, G. D.; Schüth, F. *Science* **1996**, *273*, 768. (b) Yang, H.; Vovk, G.; Coombs, N.; Sokolov, I.; Ozin, G. A. *J. Mater. Chem.* **1998**, *8*, 743.

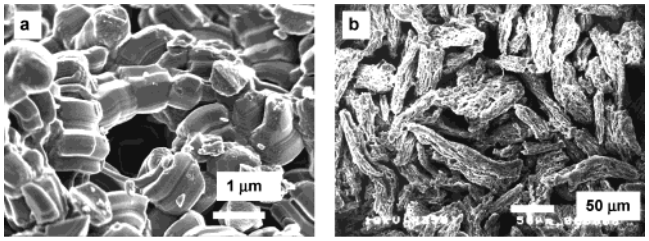

Figure 4. FE-SEM micrographs of the products using H_2SO_4 as an acid source (a) without stirring and (b) with stirring.

resulted in neither the well-defined rodlike nor the fiberlike products. It was observed, however, that the different counterions of these acids had a large effect on the macroscopic morphology of the products of these reactions. SEM images indicated that these other products obtained using various acid sources were the result of rapid silica sedimentation, meaning rapid formation of the solid product from the mixture, which does not yield rodlike particles, the basic structural unit of the products in this study, regardless of induction time.

HNO_3 and HBr had induction times comparable to those for HCl (listed in Table 1). When HNO_3 and HBr were used, the formation of aggregates of nearly spherical particles under static conditions and the slight elongation of these aggregates upon stirring were observed, reflecting rapid silica precipitation immediately after induction time (Supporting Information, Figure S-4). H_2SO_4 was an exception, having an induction time of only 30 s. In other aspects, such as the progression of silica condensation and solid-phase sedimentation, H_2SO_4 was similar to the reactions using HCl. Parts (a) and (b) of Figure 4 show the silica products formed using H_2SO_4 as an acid source without and with stirring, respectively. Loosely agglomerated rodlike particles ca. 1 μm in size can be seen in Figure 4a. Stirring during the reaction was found to induce the formation of slightly elongated silicas (Figure 4b). Surprisingly, the product in Figure 4b has the same rodlike microstructure as that seen in Figure 1e (Supporting Information, Figure S-1(d)). The XRD and sorption isotherms (Supporting Information, Figures S-5 and S-6) indicate that the sample prepared using H_2SO_4 without stirring contains relatively well-ordered mesostructures. The porous properties of samples prepared using HNO_3, HBr, and H_2SO_4 are also listed in Supporting Information, Table T-1.

Microporosity and Pore Size Distribution. As described in Table 1, the t-plots[24,26−28] confirm that almost all fiberlike silicas tend to have larger micropore volumes than rodlike silicas synthesized under the same reaction conditions excluding the use of stirring. Figure 5 shows the relationship between the S_{BET} and micropore volume for the products, some of which are not listed in Table 1. As can be seen in Figure 5, a strong correlation exists between the two. This relationship indicates that the differences in S_{BET} between products obtained using the same mixing ratio with or without

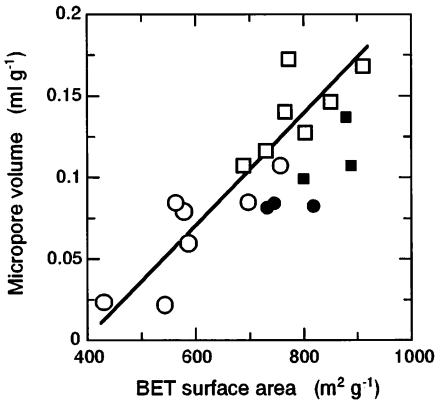

Figure 5. Relationship between S_{BET} and the micropore volume for products obtained at various reaction conditions without stirring (circles) and with stirring (squares), some of which were not listed in Table 1. Closed marks indicate products obtained using HNO_3, HBr, and H_2SO_4 in place of HCl as an acid source.

stirring are attributable to micropore quantity. However, the micropore volume of rodlike particles increases over 0.1 mL/g with an increase in the amount of HCl in the reaction (samples RC and RG).

The BJH pore size distribution curves of various rodlike and fiberlike samples (Supporting Information, Figure S-7) showed a narrow pore size distribution around a diameter of 5−7 nm for both products. Moreover, as Table 1 shows, mean pore diameters were nearly identical for the products prepared with equal reactant-mixing ratios irrespective of stirring.

Poly(ethylene oxide), as a hydrophilic block, leads to additional microporosity in the silica walls of mesoporous SBA-15 as a result of molecular templating of single EO chains.[26−29] The identical mesopore size along with the larger micropore volume of fiberlike silica compared to the rodlike silica described above would indicate that shearing flow leads to EO block extension and diffusion within the crystalline structure in keeping the size of the hydrophobic core comprised predominantly of PO blocks.[3,5,30] Furthermore, a larger concentration of HCl increases the hydrophilicity in EO moieties, favoring a stronger interlinkage of hydrophilic EO blocks with silica species during solidification, possibly leading to easier formation of micropores in the silica walls.

In our experiments, we could control the pore size between 5.6 and 6.7 nm only for fiberlike silicas with a well-defined macroscopic morphology by changing the reaction temperature in the range of 30−40 °C. However, pore sizes of rodlike silicas were difficult to control while maintaining monodispersed morphologies. The increase in pore size with increasing reaction temperature is a characteristic feature of a block copolymer templating pathway.[26−29] Partial dehydration of PEO blocks resulting from increased reaction temperature leads to a decrease of their hydrophilic layer and an

(26) Miyazawa, K.; Inagaki, S. *Chem. Commun.* **2000**, 2121.
(27) Kruk, M.; Jaroniec, M.; Ko, C. H.; Ryoo, R. *Chem. Mater.* **2000**, *12*, 1961.
(28) Galarneau, A.; Cambon, H.; Renzo, F. D.; Fajula, F. *Langmuir* **2001**, *17*, 8328.
(29) Clere, M. I.; Davidson, P.; Davidson, A. *J. Am. Chem. Soc.* **2000**, *122*, 11925.
(30) (a) Kleppinger, R.; Mischenko, N.; Theunissen, E.; Reynaers, H. L.; Koch, M. H. J.; Almdal, K.; Mortensen, K. *Macromolecules* **1997**, *30*, 7012. (b) Schmidt, G.; Muller, S.; Lindner, P.; Schmidt, G.; Richtering, W. *J. Phys. Chem. B* **1998**, *102*, 507. (c) Melosh, N. A.; Davidson, P.; Feng, P.; Pine, D. J.; Chmelka, B. F. *J. Am. Chem. Soc.* **2001**, *123*, 1240.

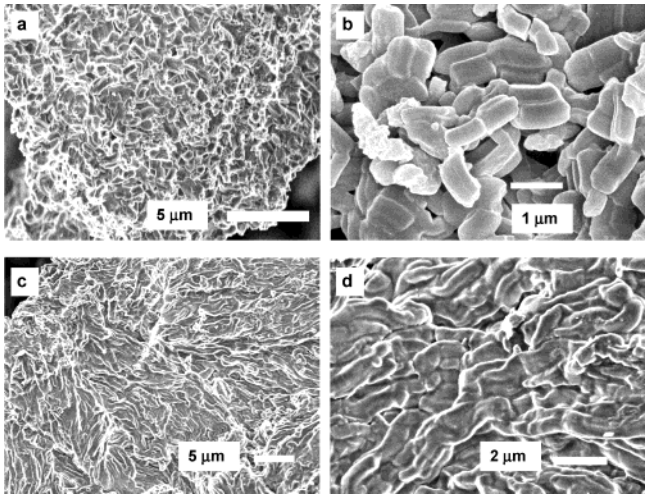

Figure 6. FE-SEM micrographs of surface textures of the products obtained for 1 h at the basic reaction conditions: (a), (b) without stirring; (c), (d) with stirring.

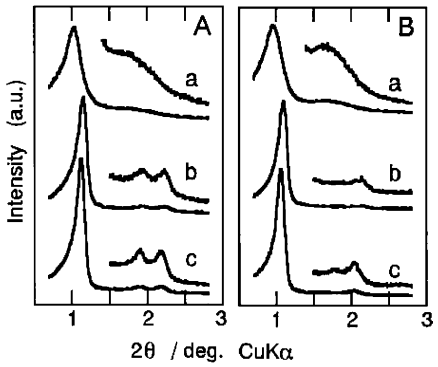

Figure 7. Powder X-ray diffraction patterns showing the time evolution of the (A) rodlike and (B) fiberlike silicas. Reaction times are (a) 1 h, (b) 3 h, and (c) 6 h. A part of the pattern for all samples is drawn at five magnifications.

increase in micelle diameter,[3–5] which results in increased mesopore size.

Particle Formation. Figure 6 shows the FE-SEM images of intermediate products obtained using the basic reaction mixture after 1 h. The difference in surface textures is clearly visible between (a) (without stirring) and (c) (with stirring) of Figure 6, although both products were irregular solids (Supporting Information, Figure S-8). Densely aggregated solids obtained under static conditions (Figure 6a) are composed of numerous rodlike particles (Figure 6b). In Figure 6c, however, the trace of many continuous structures can be seen on the surface of the product prepared with stirring. Further, Figure 6d shows a magnified image of those surfaces, exhibiting a connected structure of uniform rodlike particles fused together. Fiberlike products observed after 3 h had almost identical morphology to that after 6 h (Figure 1b), whereas products obtained after 3 h under static conditions were loosely packed solids consistent with rodlike particles (Supporting Information, Figure S-8).

Figure 7 shows the XRD patterns of products without and with stirring for 1, 3, and 6 h. Sorption isotherms and pore size distribution curves of corresponding samples are shown in Figure 8 and Figure 9, respectively. Irrespective of stirring conditions, these results, XRD, isotherms, and pore size distributions, for the

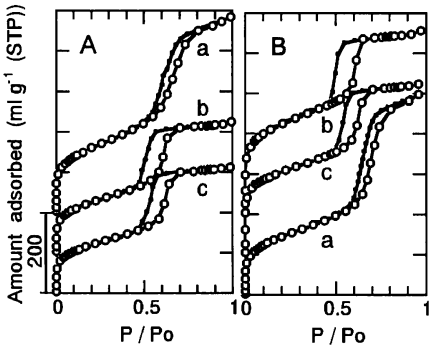

Figure 8. Nitrogen sorption isotherms showing the time evolution of the (A) rodlike and (B) fiberlike silicas. Reaction times are (a) 1 h, (b) 3 h, and (c) 6 h. Open, adsorption; closed, desorption. Isotherms are offset by 100 mL/g for clarity.

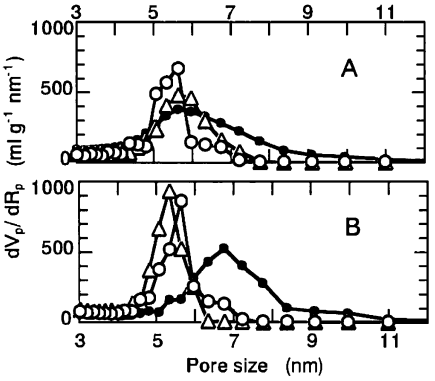

Figure 9. BJH pore size distribution curves showing the time evolution of the (A) rodlike and (B) fiberlike silicas. Reaction times are (●) 1 h, (△) 3 h, and (○) 6 h.

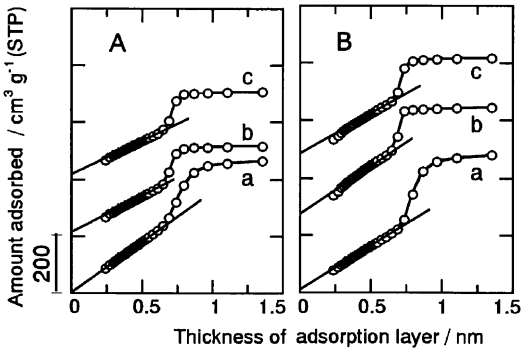

Figure 10. t-plots of nitrogen adsorption isotherms showing the time evolution of the (A) rodlike and (B) fiberlike silicas. Reaction times are (a) 1 h, (b) 3 h, and (c) 6 h. The t-curves are offset by 200 mL/g for clarity.

products for 1 h are markedly different from the patterns of the products for 3 and 6 h. Both products exhibit an enlargement and broadening of the (100) reflections along with poorly resolved higher angle peaks and, consequently, broader pore size distributions. In addition, Figure 10 shows the t-plot curves, in which the intercept of the extrapolated linear region almost reaches the origin for both 1-h samples. This indicates that the samples prepared for over 3 h with stirring have a relatively large number of micropores, whereas the products obtained using very short stirring times have few micropores. Table 2 summarizes the physicochemical parameters of the intermediate phases, including the final products RA and FA.

Table 2. Evolution of Physicochemical Properties as a Function of Reaction Time

reaction time (h)	stirring state	S_{BET} (m^2/g)	V_{meso} (mL/g)	V_{micro} (mL/g)	D_{meso} (nm)	d_{001} (nm)	particle morphologies
1	without	577	0.65	0	5.80	8.49	solid
3	without	449	0.66	0.01	5.80	7.67	loosely aggregated solid
6 (RA[a])	without	430	0.46	0.02	5.46	7.89	monodispersed rod
1	with	521	0.47	0.01	6.75	9.11	solid
3	with	805	0.66	0.11	5.33	8.03	fiber
6 (FA[a])	with	730	0.63	0.12	5.62	8.27	fiber

[a] Sample names shown in Table 1. All notations are consistent with those in Table 1.

These experimental results indicate that the products formed after 1 h are comprised of rodlike particles with less-ordered mesophase structures, indicating the initial formation of flexible, cylindrical silicated-surfactant micelles. Silica networks might become heavily cross-linked together with gradual rearrangement into a hexagonal stacking pattern of cylindrical micelles through the polymerization of silica species on irregular arrays of cylindrical micelles.

On the other hand, the macrostructural evolution appears to occur from the short connections between fused rodlike particles with disordered mesophases (Figure 6c,d) to long, well-defined fiberlike silicas composed of connected, but distinct, rodlike particles (Figures 1b and 2e). This implies that rodlike particles, formed independently at an earlier stage, immediately agglomerate as a result of shearing flow. Variously sized fiberlike silicas, all of which have the same size as rodlike primary particles (Supporting Information, Figure S-1), form in a wide range of synthesis conditions with stirring, even where agglomerated short rodlike particles form without stirring (Table 1). Shearing flow should lead to more pronounced intermicelle correlations[5,30] and eventually induce the elongation of short cylindrical silicated-surfactant micelles along the flow direction with continuous stirring. Both shearing flow and numerous elongated cylindrical silicated-surfactant micelles formed by stirring are necessary factors for the formation of fiberlike silicas comprised of bundles of fibers.

On the other hand, the SEM images indicate that the evolution of the texture as a function of the synthesis duration seems to be explained neither by the respective simple gradual transformation of rodlike products nor by the simple shearing effect on fiberlike products as mentioned above. Some rearrangement accompanied by a partial dissolution would have to occur during the formation of the initial, less-ordered mesophase structures into the highly ordered, hexagonally stacked mesostructures of the monodispersed final products.

Conclusions

A one-step selective synthesis approach of rodlike and fiberlike SBA-15 with well-defined morphologies and high mesoscopic ordering using a commercial sodium silicate solution and P123 triblock copolymer in acidic solution was performed. These morphologies varied according to slight changes in experimental conditions such as shearing flow, reactant mixing ratio, temperature, and acid source. Monodispersed rodlike silicas with ca. 0.5-μm width and 1−2-μm length were prepared under a very limited range of synthesis conditions without stirring. On the other hand, fiberlike silicas with various lengths of 20 μm to several hundred micrometers were obtained from a relatively wide range of synthesis conditions with stirring. The coupling of the rodlike particles lead to the fiberlike products in every experiment in this study.

Although rodlike and fiberlike mesoporous silicas have been previously synthesized using a low-cost inorganic silica source, we have obtained rodlike silicas as monodispersed particles, fiberlike particles with controllable length and pore size, and a further simplified synthesis procedure. We believe that our SBA-15 products would be ideal "nanoreactors" or members of a "nanoproduction facility" for making uniform nanowire and nanotube and fiberlike materials of carbon,[31] metals,[32] polymers,[33] and other products.

Acknowledgment. The authors would like to thank Prof. Kuroda of Waseda University for his critical reading and fruitful comments of this manuscript. We are grateful to Dr. Y. Soneda, Dr. M. Kodama, and technical stuff Ms. M. Jona (Institute for Energy Utilization, AIST) for their helpful FE-SEM observation.

Supporting Information Available: SEM, FE-SEM micrographs, XRD patterns, sorption isotherms of N_2, and BJH pore size distribution curves, and additionally, the porous properties listed in the table (PDF). This material is available free of charge via the Internet at http://pubs.acs.org.

CM030622U

(31) Ryoo, R.; Joo, S. H.; Kruk, M.; Jaroniec, M. *Adv. Mater.* **2001**, *13* (9), 677. Kim, S. S.; Pinnavaia, T. J. *Chem. Commun.* **2001**, 2418.

(32) (a) Han, Y. J.; Kim, J. M.; Huang, M. H.; Stucky, G. D. *Chem. Mater.* **2000**, *12*, 2068. (b) Choudrey, A.; Yang, P. *Chem. Commun.* **2000**, 1063. (c) Fukuoka, A.; Sakamoto, Y.; Guan, S.; Inagaki, S.; Sugimoto, N.; Fukushima, Y.; Hirahara, K.; Iijima, S.; Ichikawa, M. *J. Am. Chem. Soc.* **2001**, *123*, 3373.

(33) Kageyama, K.; Tamazawa, J.; Aida, T. *Science* **1999**, *285*, 2113.